Hybrid graphene-decorated metal hollow fibre membrane reactors for efficient electro-Fenton - Filtration co-processes

Thi Xuan Huong Le, Ludovic Dumée, Stella Lacour, Matthieu Rivallin, Zhifeng Yi, Lingxue Kong, Mikhael Bechelany, Marc Cretin

Hybrid graphene-decorated metal hollow fibre membrane reactors for efficient electro-Fenton - filtration co-processes

Thi Xuan Huong Le[1], Ludovic F. Dumée[2*], Stella Lacour[1], Matthieu Rivallin[1], Zhifeng Yi[2], Lingxue Kong[2], Mikhael Bechelany[1*], Marc Cretin[1*]

[1]Institut Européen des membranes, IEM UMR-5635, Université de Montpellier, ENSCM, CNRS, Place Eugène Bataillon 34095 Montpellier cedex 5 FRANCE.

[2]Deakin University, Geelong, Institute for Frontier Materials, Waurn Ponds, 3216, Victoria, AUSTRALIA.

* Corresponding authors:

ludovic.dumee@deakin.edu.au, mikhael.bechelany@umontpellier.fr and marc.cretin@umontpellier.fr

ABSTRACT

Metal hollow fibre membranes offer excellent chemical and mechanical stability and are promising platforms for the removal of harsh contaminants from solutions. Stainless steel (SS) membranes are however prone to oxidation and advanced decoration routes are required to passivate the surface of such materials. Here, SS membranes were modified with nanoscale coatings of graphene to promote electrochemical reactions and prevent premature corrosion of the bare metal reinforcement upon electro-Fenton (EF) reaction. Samples decorated with graphene oxide or reduced graphene oxide were compared to bare SS membranes to assess the impact of graphitization on the electrochemical performance of the membranes. Membranes properties were characterized using both cyclic and linear scanning voltammetry. The results evidenced that electron transfer kinetics were significantly enhanced on the reduced graphene oxide, compared to raw material. In addition, the removal efficiency of a pharmaceutical pollutant, paracetamol, was evaluated in electro-Fenton batch experiments, on the three membrane electrodes. The best mineralization current efficiency at 37 % was found when using reduced graphene oxide membrane cathode at optimal applied potential of -0.5 V *vs.* SCE (Saturated Calomel Electrode). Finally, the coupling of electro-Fenton and filtration processes was carried out on a pilot-scale unit. Various electrochemical and hydrodynamic parameters that affect mineralization efficiency were studied. By coupling filtration and electrochemical processes, the mineralization current efficiency value was increased remarkably by 165 % and remained stable for three consecutive cycles. This strategy opens up opportunities to generate low cost catalytic membrane reactors with high flux and selectivity from the materials reactivity as opposed to sieving, with potential for harsh chemicals mineralization.

Keywords

Electro-Fenton process, mineralization current efficiency, metal hollow fibre membrane, reduced graphene oxide coating, hybrid membrane process

Graphical abstract

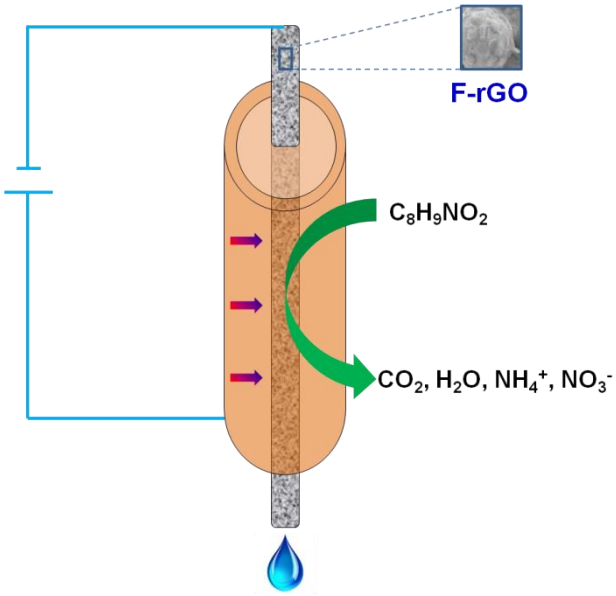

1. Introduction

Electro-Fenton (EF) processes are considered as some of the most efficient technologies to remove organic pollutants effectively from wastewater[1]. EF reactions lead to the production of powerful oxidizing agents, such as hydroxyl radical (•OH), which can attack and mineralize organic compounds as well as their by-products in short time-scales, making the process cost-effective and up-scalable[2].

In order to improve the electrocatalytic activity of the cathode materials and to increase the electron transfer kinetics of the oxygen reduction reaction (ORR), advanced materials and specific surface modification methods were successfully developed[3]. Multi-walled carbon nanotubes[4], nitrogen functionalized carbon nanotube[5], ethanol/hydrazine hydrate[6] and polymers[7],[8] were used as substrates to generate EF electrodes. Recently, graphene has become a material of choice as a modifier for enhancing electrochemical performances of electrodes for its high specific surface area and tunable conductivity[9],[10]. Carbon felt (CF) cathodes decorated with graphene were found to produce more •OH radicals during the EF reaction than their counterpart based carbon felts with an increase of 19% in mineralization reached for Acid Orange 7, an azo-dye pollutant[11]. Additionally, graphene@graphite-based gas diffusion electrodes were shown to offer a more than 3 times higher electrical conductivity compared to bare graphite particles, supporting the electrocatalytic degradation of Rhodamine B by EF process. The kinetics of H_2O_2 generation was accelerated and the electron transfer number linked to the ORR calculated at around 2.1 - 2.2[12]. Carbon fiber brush cathodes, coated with graphene, increased comparatively the H_2O_2 yield by 40% compared to uncoated electrodes and favored the EF mineralization of phenols by 20.5 %[13]. A key limitation remaining in the design of advanced EF system lies in the increase of the contact surface to favour higher kinetics of contaminants removal. Coupling cathodic electro-Fenton reaction to membrane filtration was then proposed to

enhance AO7 degradation compared to batch experiments [14]. Unfortunately AO7 mineralization rate was poor because of the low H_2O_2 production rate. In this way, by coupling cross-flow electro-Fenton on carbon membrane to anodic oxidation (AO) on Ti4O7, enhanced mineralization rates were obtained for bio-refractory pollutants [15] thanks to the contribution of AO.

Graphene has been applied across the surface of metal based materials, including highly porous materials, to develop anticorrosive capabilities[16]. The electro-deposition of graphene in highly ionized solutions allows for the decoration with nanoscale coatings from graphene precursors, such as graphene oxide, leading to a range of hydrophobicity and surface properties[17]. The tuning of the electrical properties and surface charge of graphene can further facilitate redox reactions typically occurring across metal surfaces, while avoiding oxidation of the metal[18]. The application of graphene coatings across porous metals[19] naturally sensitive to corrosion mechanisms is critical to applications such as adsorption, catalysis or separation, where high surface to volume ratio are required.

Various EF pilots were designed towards the practical application to treat large volumes of wastewater generated from industrial plants. Dichlorofenac, an organic micro-pollutant, present in drinking water could be degraded efficiently in an EF filter pilot with capacity of 200 L, and the mineralization current efficiency (MCE) attained over 20%[20]. In order to decrease energy consumption, solar photoelectro-Fenton (SPEF) pre-pilot plants were able to produce an average current of 5.0 A to mineralize Yellow 4 diazo-dyes[21], antibiotic chloramphenicol[22], or sulfanilamide[23]. However, designing efficient pilots with high mineralization capacity remains a difficult challenge and combinatorial solutions involving coupling technologies such as catalysis and adsorption or membrane separation have a clear potential[24].

In this study, hybrid separation electro-Fenton catalysts were generated by electrodeposition and reduction of graphene oxide across the surface of the pores of pre-formed stainless steel (SS) hollow fibre (HF) membranes[25]. The electrochemical properties of the hybrid membranes were characterized using the cyclic voltammetry (CV) technique with ferrocyanide system and measurement of the peak current of $Fe(CN)_6^{3-/4-}$. The ORR was confirmed by linear scanning voltammetry (LSV) analysis. The degradation efficiency of paracetamol (PCM) was evaluated in EF batch experiments, while a pilot was designed in order to remove PCM by coupling the filtration ability offered by the metal membranes to the EF process. This strategy opens new avenues for the design of catalytic membrane reactors with sieving and mineralization capabilities from the high electrical conductivity and surface area generated by the graphene coatings.

2. Experimental

2.1. Materials

Potassium hexacyanoferrate ($K_4[Fe(CN)_6]$, ≥ 99%, CAS 13746-66-2) and potassium nitrate (KNO_3, ≥ 99%, CAS 7757-79-1) were bought from Fluka. Paracetamol (PCM reagent grade, CAS 103-90-2), sodium hydroxide (NaOH, 99%, CAS 1310-73-2), sulphuric acid (H_2SO_4, 95–97%, CAS 7664-93-9), anhydrous sodium sulphate (Na_2SO_4, 99.0–100.5%, CAS 7757-82-6), iron (II) sulphate hepta-hydrate ($FeSO_4.7H_2O$, 99%, CAS 7782-63-0) were purchased from Sigma-Aldrich and used without farther purification.

Relevant chemicals for the graphene oxide synthesis were sourced and used as from previous reports[26] by the modified Hummer's method. For the deposition, a 5 wt% solution of graphene oxide was used with a 10 mM NaCl solution at 1:1 (Analytical grade, 99.99%, CAS 7647-14-5) as an electrolyte. The SS HF membranes were sourced from the company AMS (Adelaide, Australia), and were referenced as microfiltration membranes given their pore size distribution in the micron range.

2.2. Preparation of hybrid hollow fibre membranes

The coating of graphene oxide (GO) across the SS membranes was performed following an electrophoretic deposition (EPD) process as previously described (Figure S1)[17]. The SS membrane (length of 15 cm) was washed with ethanol and acetone in an ultrasonic water bath to remove any impurities and blow dried with nitrogen gas. The concentration of GO suspension was adjusted to 0.5 $mg.mL^{-1}$. EPD was carried out with SS tube as working electrode (anode) and titanium foil as counter electrode (cathode). GO was coated onto SS tube for 1 min. at 10 V with a working distance of 1 cm. After EPD, the sample was removed from the GO suspension and dried with a hot air gun and stored at room

temperature. The GO coated on SS membranes were reduced with hydrazine hydrate vapor in an autoclave at 90°C for 10 h following a procedure previously developed[19].

2.3. Materials characterization

2.3.1. Physical characterization

Scanning electron micrographs (SEM) were acquired on a JEOL 7800F FEG-Scanning Electron Microscope (Japan). The tests were performed on uncoated samples as provided with a 5 keV accelerating voltage and at a distance of 10 mm. Raman spectra were acquired on an inVia Raman microscope (Renishaw, United Kingdom) at a laser wavelength of 514 nm. An extended scan ranging from 100 to 4000 cm^{-1} was performed for 10 s with laser power of 25 mW. The bubble point, average pore size and pore size distribution of the metal HFs were measured using a porometer (Porometer 3GZH Quantachrome Instruments, USA) after wetting the HFs with Porofil® as a wetting solution (16.00 $dyn.cm^{-1}$ surface tension). Porosity of the bare SS HF membranes was evaluated by liquid porosimetry following a previously described protocol[25]. The mechanical properties of the SS HF membranes including Young moduli, tensile and breaking strengths were determined on an Instron instrument (Instron Corporation, USA) fitted with a 30 kN static load cell at pulling speed of 10 $mm.min^{-1}$. The tensile strength tests were carried out three times using 5 cm long samples to evaluate the repeatability of the experiments.

2.3.2. Electrochemical characterization

The electrochemical characterization of prepared membranes (2 cm height x 0.5 cm diameter) were performed by running cyclic voltammetry (CV) curve in a three-electrodes cell containing solution of 10 mM $K_4[Fe(CN)_6]$ and 1.0 M KNO_3 which was connected to a µ3AUT70466 Autolab system (Eco Chemie BV, Netherlands). This cell consisted a working

electrode (F, F-GO, F-rGO), a counter electrode (Pt foil), and a reference electrode (Saturated Calomel Electrode, SCE). The CV experiments were performed at various scan rates including 3, 5, 10 and 20 mV s^{-1}.

In order to evaluate the catalytic activity of fabricated membranes towards the ORR, linear scanning voltammetry (LSV) was used to observe the oxygen reduction. This experiment was conducted under both nitrogen and oxygen atmosphere using a μ3AUT70466 Autolab device from the open circuit potential to -2.0 V *vs* SCE at a scan rate of 5 mV s^{-1}.

The three-electrode cell was also used with an aqueous solution of 25 mL Na_2SO_4 (50 mM) that was adjusted at pH 3.0 with sulfuric acid (1 M). Prior to the experiment, oxygen was bubbled during 30 min and kept constant during cell running. All experiments were carried out at room temperature, and all the potential values presented in this study were referred to SCE.

2.4. Removal of PCM in EF batch experiments

The paracetamol (PCM) mineralization efficiency of the three prepared membranes, bare SS, graphene oxide SS, and reduced graphene oxide metal membranes was investigated by performing the EF batch experiment in an undivided cylindrical glass cell equipped with two electrodes.

The membranes (2 cm height x 0.5 cm diameter) were used as working electrode and a Ti grid as auxiliary electrode which was placed parallel and at a distance of 3 cm from the working electrode. A solution containing 50 mL of PCM (0.1 mM), $FeSO_4.7H_2O$ (0.2 mM) as the catalyst and Na_2SO_4 (50 mM) as supporting electrolyte was prepared for batch experiment. The solution pH was adjusted at 3.0, magnetically stirred at 800 rpm and saturated with oxygen bubbling prior and during the electrolysis. Constant value of potential was applied between the working and the auxiliary electrodes using chrono-amperometry

mode from μ3AUT70466 Autolab system (Eco Chemie BV, Netherlands). In the case of F-rGO membrane electrode, three difference of potentials were applied (-0.1 V, -0.5 V and -1.0V). Then, -0.5 V was selected to do a comparison test for F and F-GO membrane cathodes.

The TOC of the samples was measured by a TOC-L CSH/CSN Shimadzu (Japan) analyzer. The measured results allowed to calculate the mineralization current efficiency (MCE) from Eq. 1[27]:

$$\text{MCE (\%)} = \frac{\text{n F V}_\text{s} \Delta(\text{TOC})_{\text{exp}}}{4.32\times10^{7}\text{m Q}} \times 100 \quad (1)$$

where n is the number of electrons consumed in the mineralization of each PCM molecule, F is the Faraday constant (96485 C mol^{-1}), V_s is the solution volume (L), $\Delta(TOC)_{exp}$ is the experimental TOC decay (mg L^{-1}), 4.32×10^7 is a conversion factor (3600 s h^{-1} × 12000 mg carbon mol^{-1}), m is the number of carbon atoms in the PCM molecule (8 atoms), Q is the charge (C) passing through the system. The number of electrons (n) consumed for mineralization was 34 for the PCM molecule, according to the stoichiometry of the reaction of Eq. 2:

$$C_8H_9NO_2 + 14H_2O \rightarrow 8CO_2 + NH_4^+ + 33H^+ + 34e^- \quad (2)$$

2.5. Pilot-unit for coupling filtration and EF process to degrade PCM

A pilot-unit was designed as in Figure S2 for coupling filtration and EF process for the removal of PCM in aqueous medium. The F-rGO cathode with dimension of 14.2 cm height x 0.5 cm diameter was placed in the center of the reactor and cylinder stainless steel (SS) anode surrounded the cathode. The applied voltage was supplied from a generator (Lambda Electronique, USA). The flow rate (D1) of the feed solution was fixed at 1.7 L h^{-1}. The oxygen gas supply was used to adjust the transmembrane pressure ΔP. Oxygen gas fulfills therefore two functions: adjust the permeation rate and saturate the solution to produce hydrogen peroxide (H_2O_2) by EF reaction. The temperature of the solution in the reactor was

maintained at a fixed value using a thermostatic control system (Thermo-chiller HRSE024-A-23). The permeate flux was determined by measuring the mass of solution going out the outlet using an automatic balance (Adam HCB 1002) connected to a computer.

Permeability of the membrane was preliminary estimated on ultra-pure water solution under different transmembrane pressure conditions. Then, water was replaced with PCM pollutant in solution (0.1 mM in electrolyte). In order to estimate possible retention phenomena of PCM occurring on the membrane, pilot-unit experiment was carried out without applying any current. Total organic carbons (TOC) of the collected permeate was analyzed as a function of time using TOC-L CSH/CSN Shimadzu (Japan) analyzer.

Filtration/EF coupling experiments were then carried out on 2.5 L of the solution of PCM (0.1 mM), Na_2SO_4 (50 mM) and $FeSO_4$ (0.25 mM), saturated with O_2, adjusted at pH 3.0, at feed flow rate of 1.7 L h^{-1} and transmembrane pressure ΔP = 0.16 bar, under a difference of potential of 0.5V corresponding to a current of 170 mA. Experiments were repeated for five cycles of treatment with the same electrodes and the permeate flux was checked every cycle. Between two experiments, the pilot was cleaned twice with 2.5 L H_2O during 15 min to remove any residuals inside the pilot and the membrane. To quantify the PCM degradation by anodic oxidation reaction involved on the SS anode, batch experiment was simply performed in an external glass cell.

3. Results and discussion

3.1. Physical characterization

The SS HF membranes were first examined by SEM to visualize the deposition of GO and rGO as well as to determine its impact on surface pore size. As shown in Figure 1, the SS HF membranes were composed of sintered SS particles with an average size of 10 µm. This structuring induced a relatively rough surface finish, with peak to crest values of about 20-40 µm, due to the neck formation during the sintering process and to partial particle coalescence. The HF also exhibited an inner and outer diameter of 4.8 and 6 mm respectively corresponding to a wall thickness of 600 µm, and an overall porosity of 45% for a mean pore size distribution, measured by perm-porosimetry of 1.9 µm, making them extremely mechanically resilient but yet highly permeable to liquids. In addition, the pore size distribution of the membranes was found to be narrow, ranging from 1.5 to 3.5 µm (Figure 2a). The stress at break of the HFs was found to lie around 162 MPa, at a strain of 0.1 %, representing an outstanding mechanical stiffness compared to polymeric and ceramic materials (Figure 2b).

The electro-deposition of the GO and rGO upon reduction was not found to affect neither the pore size distribution nor the porosity of SS HF membrane materials. The thickness of the deposition, as previously evaluated[17] was found to be on the order of 20 nm, thus being largely negligible compared to the actual physical size of the pores. Given the micron-size distribution of the pores of the microfiltration hollow fibres used here, no changes in pore diameter may be therefore detected. In addition, the electro-deposition process allowed coating conformally the inner pores and outer surface of the membranes highly homogeneously. The process is also highly efficient in terms of scalability and speed of deposition, allowing for tens of centimeter long membranes coating at once. The electro-plated GO and rGO sheets were visible from the SEMs in Figure 3 c to f. The waviness

generated from the overlapping layers was found to be homogeneous across the surface of the samples and to not be affected by the reduction process, maintaining the specific surface area of the material constant.

The transformation process from GO to rGO, corresponding to the specific reduction of hydroxyl and carboxylic groups present across the graphitic lattice of GO, is illustrated on the Raman spectra shown in Figure 4. The peak at 1350 cm^{-1} (D) is associated with nano-crystalline carbon domains, while that around 1575 cm^{-1} (G) is correlated to the presence of amorphous carbon, which are yet sp2 bonded. The ratio of the ID/IG peaks is therefore a measure of the crystallinity of the material and can be assessed to evaluate reduction or oxidation levels. In the current case, the ID/IG ratio, corresponding to the level of defective and amorphous sites across the materials, was found to decrease from 1.19 to 1.02 over the reduction process confirming that graphitization of the reduced GO is increased. This aspect is critical since the level of graphitization of the material will directly dictate the phonon-diffusion, and electrical conductivity of the graphene allotropes[18].

3.2. Electrochemical characterization

The electrochemical properties of the prepared cathodes were evaluated by CV to study the redox reactions of the couple Fe^{III}/Fe^{II} at the electrode surface, from a ferrocyanide solution. The larger the electroactive surface area of the electrodes, the higher the increase in peak current for the Fe^{III}/Fe^{II} couple should be[28]. As seen in Figure 5a, the current response measured on the membrane modified with rGO at scan rate of 5 mV s^{-1} was 1.6 times higher than that on the non-GO modified one. The GO deposition declined the redox kinetics of the Fe^{III}/Fe^{II} couple compared to both F and F-rGO electrodes since lower peak currents and larger potential gaps were observed between the anodic and cathodic peaks.The obtained results confirmed that the electrocatalytic activity was improved by rGO deposition thanks to

the large surface area and excellent conductivity of graphene-based materials[29]. The electroactive surface area of the F-rGO membrane was calculated by using the Randles-Sevcik formula (Eq. 3)[30],[31].

$$Ip = 2.69 \times 10^5 \times A \times D^{1/2} \times n^{3/2} \times \gamma^{1/2} \times C \quad (3)$$

Where A is the electrode area (cm^2); n is the number of electrons involved in the redox Fe^{III}/Fe^{II} reaction, D is the diffusion coefficient of $Fe(CN)_6^{4-}$ in solution ($cm^2.s^{-1}$), C is the concentration of $Fe(CN)_6^{4-}$ in solution ($mol.cm^{-3}$), and γ is the scan rate of the potential perturbation ($V\ s^{-1}$).

The electroactive surface area of F-rGO and F cathodes were found to be 6.11 cm^2 and 3.87 cm^2 respectively. On the other hand, the bare GO deposited samples showed the lowest electrochemical area (2.94 cm^2) due to the lower native conductivity of the defective graphitic structure, as previously mentioned in studies dealing with graphene-modification[32].

From the CV curves, the relationship between the peak current and the scan rate was extrapolated and is presented in Figure 5b for the three electrodes tested. The peak current of the F membrane was proportional to the square root of the scan rate with the highest determination coefficient (R^2 = 0.9757) obtained in comparison with R^2 =0.9448 for F-rGO. This result indicated a more homogeneous conductive surface of F than of rGO modified electrode, as evidenced by the presence of structural defects across the rGO structure stemming from incomplete GO reduction. However, the residual oxygen-rich functional groups could be beneficial when rGO-F was applied as a cathode material over the EF process since reducing slightly the surface hydrophobicity[33]. The low conductivity and disordered structure of F-GO were confirmed by the poor correlation factor obtained between current and scan rate (R^2= 0.8975).

3.3. EF batch experiment for PCM removal

The oxygen reduction reaction (ORR) was tested by running LSV from the open circuit potential to -2.0 V on F-rGO cathode under either nitrogen (N_2-saturated electrolyte) or oxygen (O_2-saturated electrolyte) atmosphere. The result, shown in Figure 6a, indicated that the O_2 reduction happened from +0.1 V to -0.70 V on F-rGO surface, with a pseudo-diffusion plateau reached at a potential between -0.70 and -0.40 V. At lower potentials, proton reduction occurred between -0.70 V and -1.20 V, at which solvent molecules started being reduced.[14] As a comparison, experiments were carried out on F and F-GO cathodes under the same conditions, in O_2-saturated electrolyte (Figure 6b). The ORR appeared severely limited and seemed to occur between -0.35 V and -0.70V on both F and F-GO electrodes. The O_2 reduction was not well separated in this case from that of the proton reaction, unlike for the F-rGO electrode. These CV and LSV results demonstrate that faster electron transfer kinetics for ORR were obtained on the F-rGO samples. The increased electrochemical activity from rGO deposition contributed significantly to improve the performance of oxygen reduction involved at the surface of the modified cathode.

From these results, three potential (-0.1, -0.5 and -1.0 V) were applied to perform the EF batch experiments on the F-rGO cathodes. During the EF process, H_2O_2 was generated by the direct electro-reduction of dissolved O_2 at the surface F-rGO cathode, according to Eq. 1 [34]:

$$O_2 + 2H^+ + 2e^- \rightarrow H_2O_2 \quad (4)$$

Then paracetamol (PCM) was degraded by the attack of hydroxyl radicals (•OH) which was produced from the reaction of iron catalyst and H_2O_2 *via* the electro-Fenton (EF) process:

$$Fe^{2+} + H_2O_2 + H^+ \rightarrow Fe^{3+} + {}^{\bullet}OH + H_2O \quad (5)$$

$$PCM + {}^{\bullet}OH \rightarrow \text{oxidation products} \quad (6)$$

Commonly, MCE was used to evaluate the mineralization efficiency in relation with consumed energy, % TOC removal and volume of treated solution[27]. Figure 6c indicated that the MCE using F-rGO cathode reached the highest value (37%) at -0.5 V which was remarkably higher than at -0.1 V (MCE = 5 %). This result confirms the LSV results from Figure 6a which showed that the ORR exhibited a maximal diffusion current at -0.70 V < E < -0.40 V). As reported in literature, the H_2O_2 production rate from ORR depends on the applied potential or current[35]. Higher reducing potential accelerated not only the O_2 reduction towards H_2O_2 formation, but also promoted the regeneration of Fe^{2+}. Consequently, more hydroxyl radicals were produced to attack PCM molecules. However, applying a too high reducing potential (E< -1.0 V) decreased mineralization efficiency (MCE = 25 %), due to the appearance side redox reactions , such as four-electron O_2 reduction and H_2 production, that competed with the EF reaction[11]. This relative energy consumption was responsible for the decrease in MCE.

The applied potential at -0.5 V was therefore selected to compare the efficiency of PCM degradation by EF batch processes using F and F-GO cathodes, as shown in Figure 6d. In accordance with electrochemical characterization results, F-rGO presented the highest MCE value at 37 % compared to 22 % and 18 % for F and F-GO, respectively. These results confirm that rGO modification significantly enhance the EF process performance.

3.4. Coupling EF process to membrane filtration in pilot-unit

With regards to future industrial application, a pilot-unit that couples EF process (using F-rGO cathode) and filtration properties for this hollow fibre membrane, was designed and tested for PCM removal. In this system, the PCM was removed by the coupling of two processes: (1) Filtration to keep PCM at the membrane and (2) EF process to decompose PCM molecules by the attack of $^{\bullet}OH$. The PCM degradation pathway and the reaction

mechanism during this process (Figure S3) were carefully studied in our previous publication and presented in supplementary information [36]. Before performing the coupling of the two processes, separate experiments were carried out with the view to estimate their individual performance, (1) H_2O flux determination, (2) anodic oxidation (AO) capability of stainless steel (SS) anode, and (3) PCM filtration performance, as it has been described in the experimental section. A high H_2O flux value was obtained at around 5,000 L h^{-1} m^{-2} (Figure 7a), due to the large porosity of the F-rGO membrane previously determined (50-55%[37]). The PCM degradation by AO process on SS anode was carried out outside the pilot plant, in a cylinder glass-cell containing 2.5 L PCM (0.1 mM), Na_2SO_4 (50 mM), without adding iron catalyst, at an applied current density of 170 mA. The result from TOC analysis suggested out that no mineralization by AO reaction occured. The PCM filtration via F-rGO membrane was finally done in the pilot-unit (2.5 L PCM (0.1 mM), Na_2SO_4 (50 mM), $FeSO_4$ (0.2 mM, pH = 3, D1 = 1.7 L h^{-1} and ΔP = 0.16 bar), with and without applying current. Comparing to the coupling result, the filtration occupied 28.6 %, proving that the EF process played a main role for PCM degradation. In pilot coupling the EF process and filtration, the MCE was calculated at 165 % which was 4.5 times higher than in EF bath experiment.

For industrial application, the stability performance of the membrane is an important parameter. Therefore, the experiment was repeated for five mineralization cycles and MCE values were calculated for every cycle. Regarding Figure 7b, a slight but continuous decrease of MCE was observed for the first three cycles (MCE from 165 % to 151 %), reaching 111 % at the fifth cycle. Interestingly, this change seemed to be intimately related to that of the measured flux through the membrane (Figure 7a). The flux decreased gradually according to the cycle of experiments, evidencing fouling phenomenon of F-rGO membrane. After the first cycle, replacing H_2O by a PCM solution (with supporting electrolyte (Na_2SO_4) and catalyst (Fe^{2+})) reduced the flux to 4500 L h^{-1} m^{-2} (Figure 7a). Then the flux value decreased gradually

to less than 3000 L h^{-1} m^{-2} after 5 cycles. Under these experimental conditions, repeating the treatment cycle intensified the fouling of the membrane and affected the filtration as well as electrochemical property of membrane for EF process, leading to lower MCE value.

The current work the first approach involving hybrid graphene / metal hollow fibre membrane for bio-refractory pollutants removal by the coupling of electrochemical advanced oxidation process and filtration. The graphene coating is not only improving the performance, as we demonstrate here, but also protects the metal from corrosion [16]. This work contributes importantly to enrich the technology as well as material for membrane science towards industrial applications in waste water treatment.

4. Conclusions

In this study, a hybrid metal-graphene membrane with controlled surface properties were synthesized and tested in a combined filtration and advanced oxidation processes for the depollution of model effluents. The rGO modification of the stainless steel hollow fibre (SS HF membrane) improved the electrochemical performance of this material by increasing its electroactive surface area of 6.1 ± 0.1 cm^2 compared to 3.8 ± 0.1 cm^2 for F cathode. The better electrocatalytic activity of F-rGO accelerated the electron transfer kinetics for Oxygen Reduction Reaction (ORR) which could shifted the starting O_2 reduction potential from -0.35 V on both F and F-GO to -0.10 V on rGO modified electrode. The applied potential at -0.50 V was found to be the optimal value for PCM mineralization by EF batch process: the F-rGO cathode showed the highest mineralization current efficiency (MCE) at 37 %.

This cathode was able to combine two functions (electrochemical and filtration properties), implemented into a pilot-unit scale, and tested to mineralize a PCM (0.1 mM) solution. The coupling process was able to increase significantly the PCM removal efficiency. The permeate flux remained almost stable over three cycles. After that, increasing the cycle number led to the fouling of the membrane. The optimization of the operating conditions (hydrodynamic optimization, rinsing and conditioning cycles), would limit this phenomenon and support longer term performance and operation.

This strategy, allowing for selectivity across large pore-sized membranes not from sieving across the pores but from the reactivity across the surface of the pores, opens up new avenues for the scalable design of advanced combinatorial electro-reactive materials for harsh effluents oxidation remediation and simultaneous filtration.

Acknowledgment

Dr. Dumée acknowledges the Australian Research Council (ARC) for his DECRA fellowship (DE180100130). Dr Francois-Marie Allioux and Dr Andrea Merenda are acknowledged for experimental support. The SS HF samples were generously provided by AMS (South Australia, Australia). The authors also acknowledge the ANFF Deakin node for support.

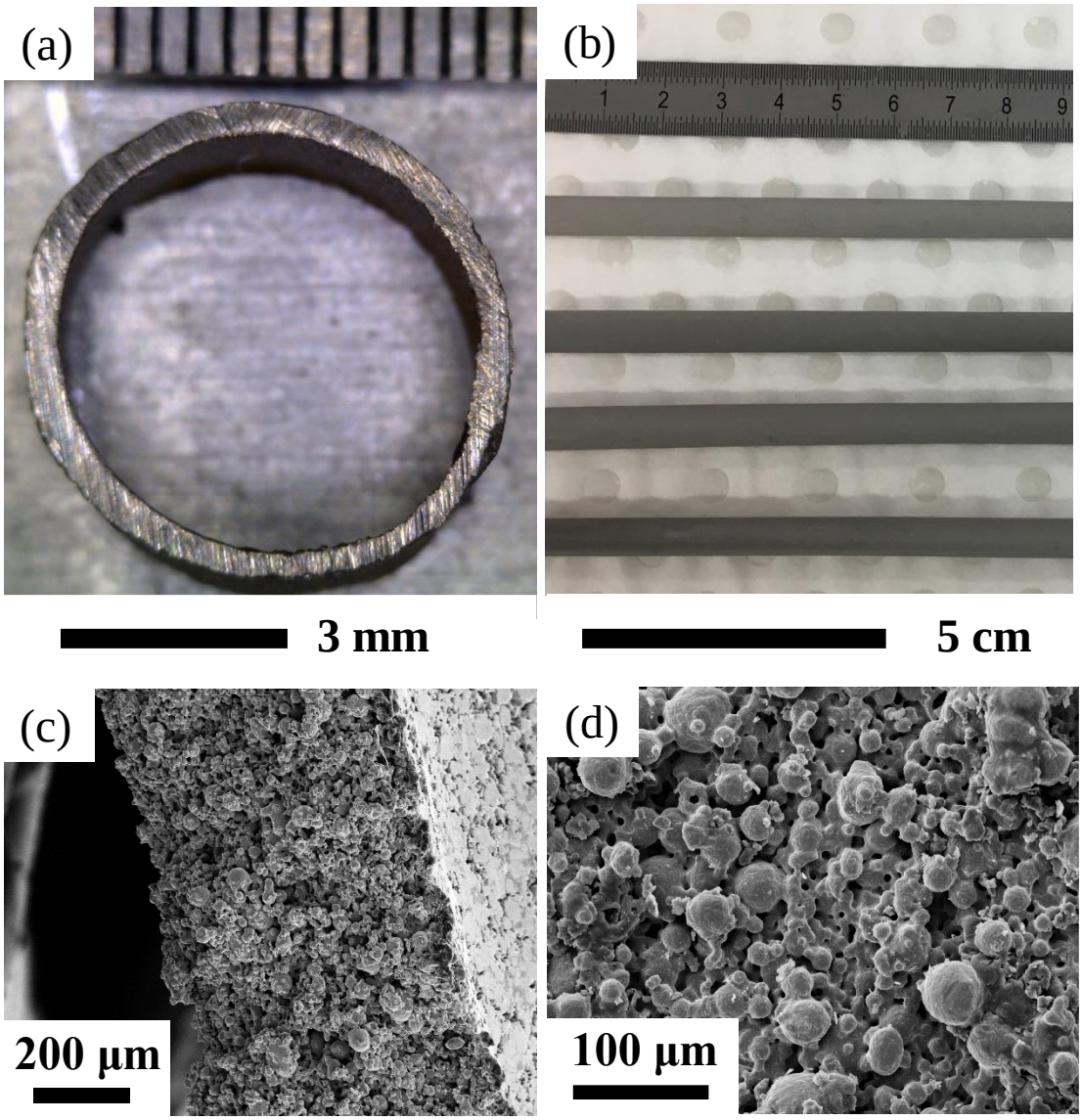

Figure 1. Cross-section optical image (a) and photograph (b) of the tubular SS substrates. (c) SEM image of the wall of the tubular substrate and (d): SEM image of the surface of the tubular substrate. The outer wall diameter was 6 mm and the thickness of the walls 620 µm +/- 15 µm.

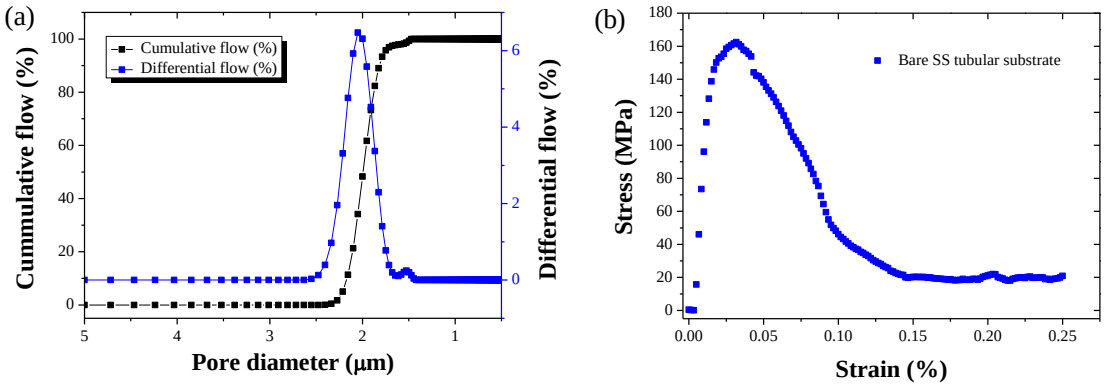

Figure 2. (a) Pore size distribution and (b) mechanical strength of the bare SS HF. The mean pore size of the bare membranes was calculated at 1.9 µm +/- 0.2 µm and the maximum flexural stress at 162 ± 15 MPa.

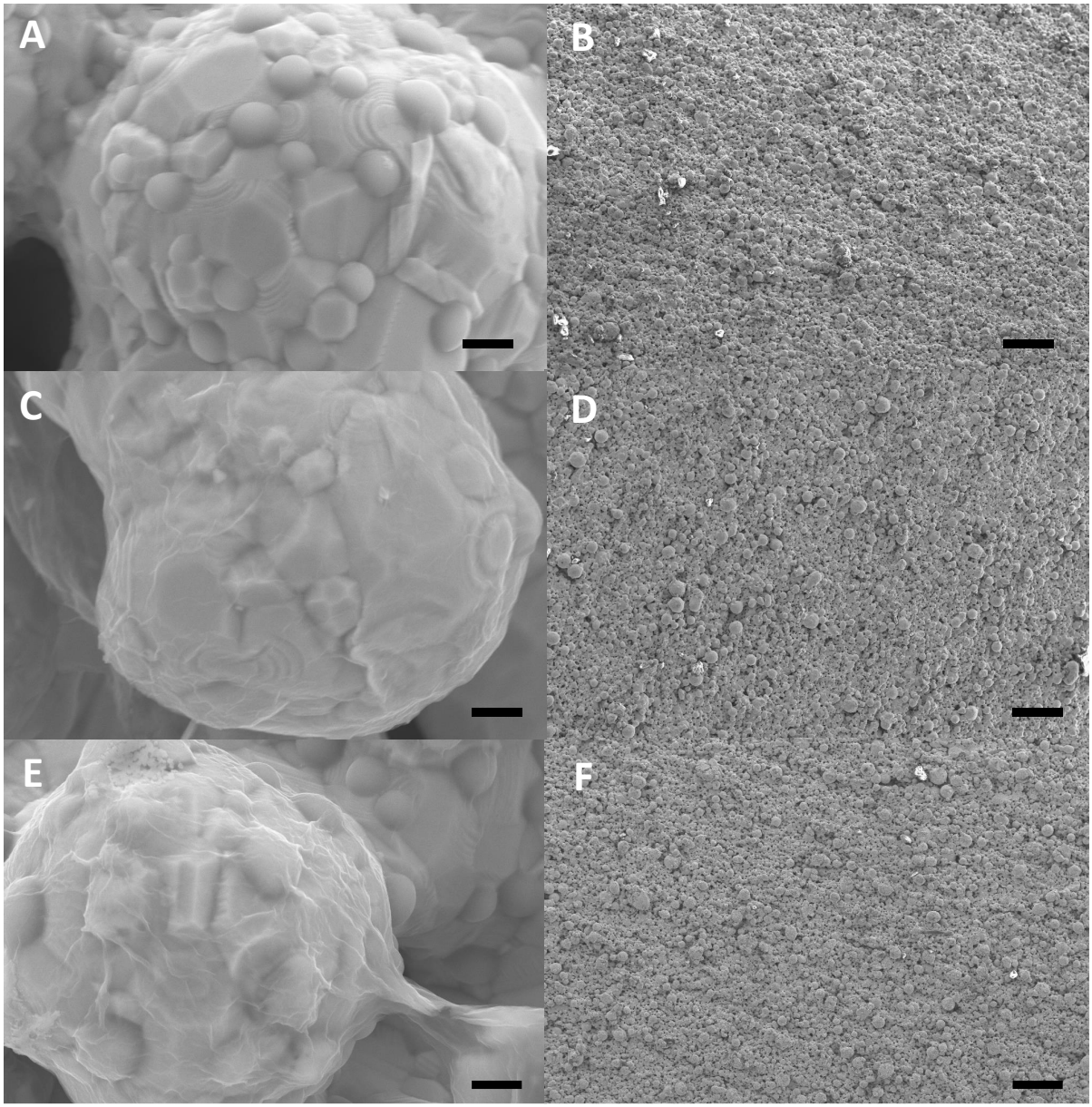

Figure 3. SEMs of the (A, B) bare SS membranes as well as (C, D) after GO and (E, F) rGO coating. The scale bars for A, C and E corresponds to 1 micrometer, while those of B, D and F to 100 micrometers.

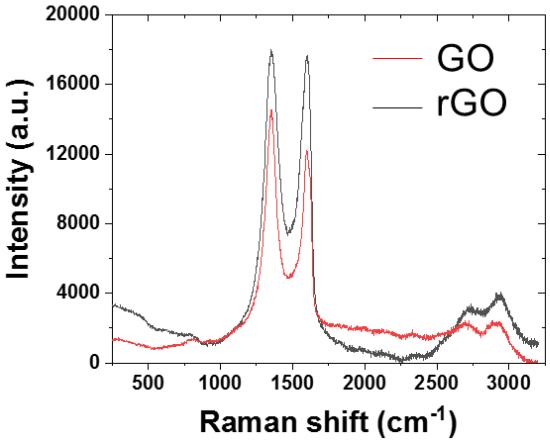

Figure 4. Raman spectra for both GO and rGO SS HF coated samples.

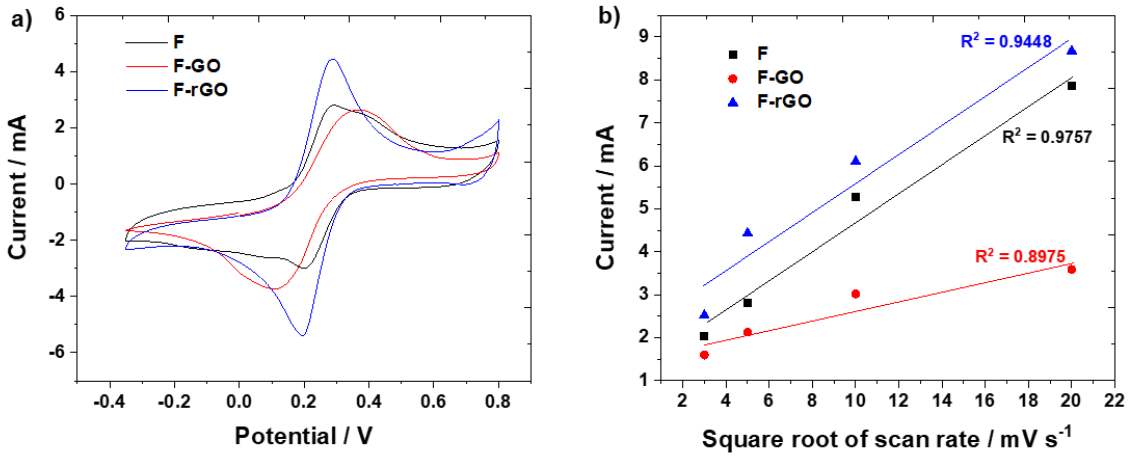

Figure 5. a) CV at scan rate of 5 mV s^{-1} and (b) the relationship between peak current and scan rate ($\sqrt{\gamma}$) of F, F-GO, F-rGO membranes.

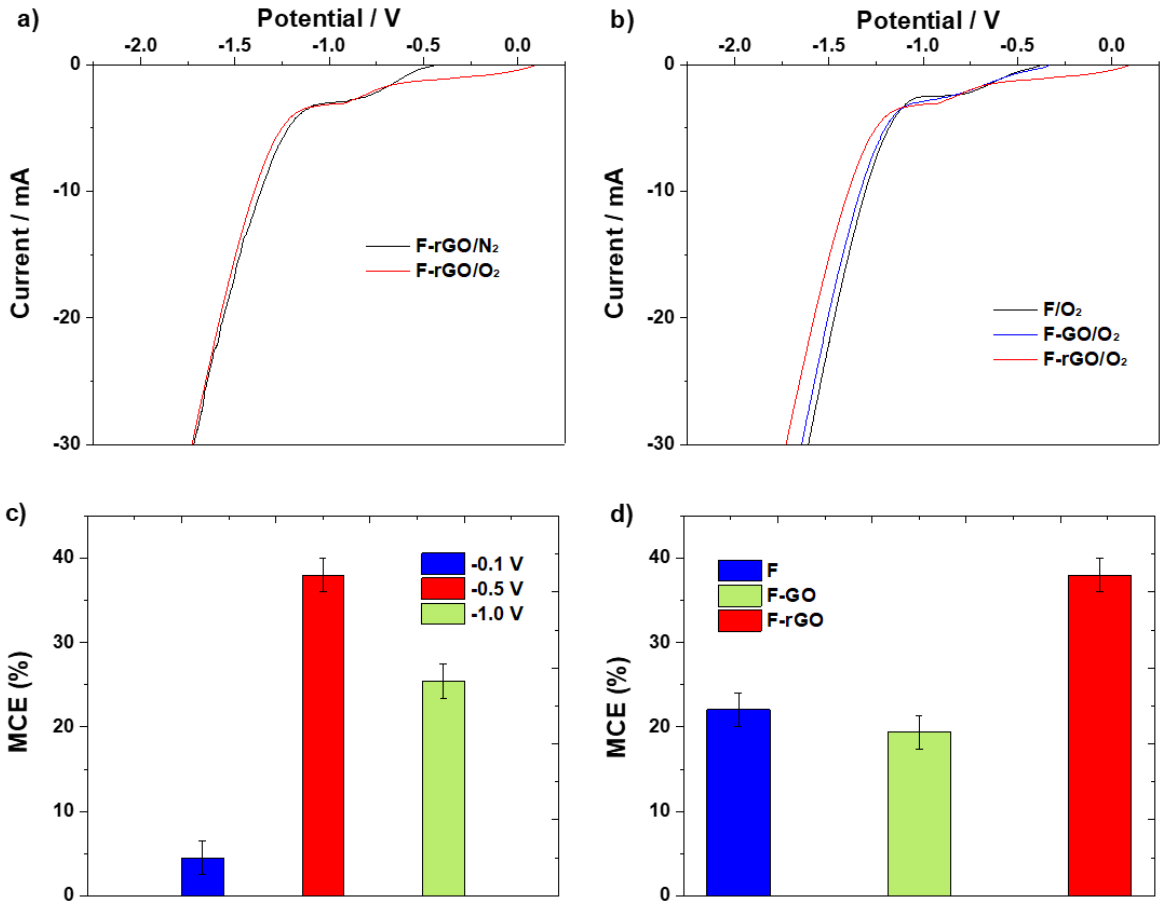

Figure 6. a) LSV of a) F-rGO under N_2/O_2 atmosphere, b) F, F-GO, F-rGO cathodes obtained in 50 mM Na_2SO_4, O_2 saturated solution, pH = 3. Scan rate 5 mV/s; MCE of PCM mineralization by EF process in bath experiment at applied potential of c) -0.1 V, -0.5 V, -1.0 V using F-rGO cathode, d) -0.5 V using F, F-FO, F-rGO cathodes.

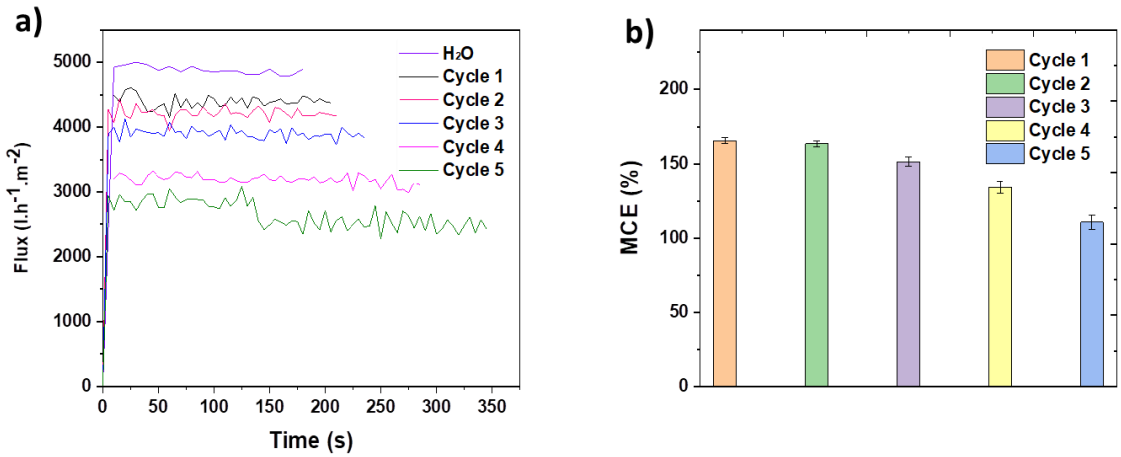

Figure 7. (a) Flux of H_2O and treated solution as function of cycle number, b) Stability of F-rGO membrane for PCM removal using pilot plant coupling EF process and filtration. $V_{solution}$ = 2.5 L, PCM (0.1 mM), Na_2SO_4 (50 mM), $FeSO_4$ (0.2 mM), pH = 3, I = 170 mA.

References

[1] E. Brillas, I. Sirés, M.A. Oturan, Electro-fenton process and related electrochemical technologies based on fenton's reaction chemistry, Chem. Rev. 109 (2009) 6570–6631. doi:10.1021/cr900136g.

[2] T.X.H. Le, T. Van Nguyen, Z.A. Yacouba, L. Zoungrana, F. Avril, E. Petit, J. Mendret, V. Bonniol, M. Bechelany, S. Lacour, G. Lesage, M. Cretin, Toxicity removal assessments related to degradation pathways of azo dyes: Toward an optimization of Electro-Fenton treatment, Chemosphere. 161 (2016) 308–318. doi:10.1016/j.chemosphere.2016.06.108.

[3] T.X. Huong Le, M. Bechelany, M. Cretin, Carbon felt based-electrodes for energy and environmental applications: A review, Carbon N. Y. 122 (2017) 564–591. doi:10.1016/j.carbon.2017.06.078.

[4] E. Pajootan, M. Arami, M. Rahimdokht, Discoloration of wastewater in a continuous electro-Fenton process using modified graphite electrode with multi-walled carbon nanotubes/surfactant, Sep. Purif. Technol. 130 (2014) 34–44. doi:10.1016/j.seppur.2014.04.025.

[5] X. Zhang, J. Fu, Y. Zhang, L. Lei, A nitrogen functionalized carbon nanotube cathode for highly efficient electrocatalytic generation of H2O2in Electro-Fenton system, Sep. Purif. Technol. 64 (2008) 116–123. doi:10.1016/j.seppur.2008.07.020.

[6] L. Zhou, Z. Hu, C. Zhang, Z. Bi, T. Jin, M. Zhou, Electrogeneration of hydrogen peroxide for electro-Fenton system by oxygen reduction using chemically modified graphite felt cathode, Sep. Purif. Technol. 111 (2013) 131–136. doi:10.1016/j.seppur.2013.03.038.

[7] G. Xia, Y. Lu, H. Xu, Electrogeneration of hydrogen peroxide for electro-Fenton via oxygen reduction using polyacrylonitrile-based carbon fiber brush cathode,

Electrochim. Acta. 158 (2015) 390–396. doi:10.1016/j.electacta.2015.01.102.

[8] G. Zhang, F. Yang, M. Gao, X. Fang, L. Liu, Electro-Fenton degradation of azo dye using polypyrrole/anthraquinonedisulphonate composite film modified graphite cathode in acidic aqueous solutions, Electrochim. Acta. 53 (2008) 5155–5161. doi:10.1016/j.electacta.2008.01.008.

[9] C.N.R. Rao, A.K. Sood, K.S. Subrahmanyam, A. Govindaraj, Graphene: The new two-dimensional nanomaterial, Angew. Chemie - Int. Ed. 48 (2009) 7752–7777. doi:10.1002/anie.200901678.

[10] S.K. Jang, J. Jeon, S.M. Jeon, Y.J. Song, S. Lee, Effects of dielectric material properties on graphene transistor performance, Solid. State. Electron. 109 (2015) 8–11. doi:10.1016/j.sse.2015.03.003.

[11] T.X.H. Le, M. Bechelany, S. Lacour, N. Oturan, M.A. Oturan, M. Cretin, High removal efficiency of dye pollutants by electron-Fenton process using a graphene based cathode, Carbon N. Y. 94 (2015) 1003–1011. doi:10.1016/j.carbon.2015.07.086.

[12] Z. Zhang, H. Meng, Y. Wang, L. Shi, X. Wang, S. Chai, Fabrication of graphene@graphite-based gas diffusion electrode for improving H2O2generation in Electro-Fenton process, Electrochim. Acta. 260 (2018) 112–120. doi:10.1016/j.electacta.2017.11.048.

[13] E. Mousset, Z. Wang, J. Hammaker, O. Lefebvre, Electrocatalytic phenol degradation by a novel nanostructured carbon fiber brush cathode coated with graphene ink, Electrochim. Acta. 258 (2017) 607–617. doi:10.1016/j.electacta.2017.11.104.

[14] P. Liang, M. Rivallin, S. Cerneaux, S. Lacour, E. Petit, M. Cretin, Coupling cathodic Electro-Fenton reaction to membrane filtration for AO7 dye degradation: A successful feasibility study, J. Memb. Sci. 510 (2016) 182–190. doi:10.1016/j.memsci.2016.02.071.

[15] H. Olvera-Vargas, J.C. Rouch, C. Coetsier, M. Cretin, C. Causserand, Dynamic cross-flow electro-Fenton process coupled to anodic oxidation for wastewater treatment: Application to the degradation of acetaminophen, Sep. Purif. Technol. 203 (2018) 143–151. doi:10.1016/j.seppur.2018.03.063.

[16] L.F. Dumée, L. He, Z. Wang, P. Sheath, J. Xiong, C. Feng, M.Y. Tan, F. She, M. Duke, S. Gray, A. Pacheco, P. Hodgson, M. Majumder, L. Kong, Growth of nano-textured graphene coatings across highly porous stainless steel supports towards corrosion resistant coatings, Carbon N. Y. 87 (2015) 395–408. doi:10.1016/j.carbon.2015.02.042.

[17] J.W. Maina, J.A. Schütz, L. Grundy, E. Des Ligneris, Z. Yi, L. Kong, C. Pozo-Gonzalo, M. Ionescu, L.F. Dumée, Inorganic Nanoparticles/Metal Organic Framework Hybrid Membrane Reactors for Efficient Photocatalytic Conversion of CO2, ACS Appl. Mater. Interfaces. 9 (2017) 35010–35017. doi:10.1021/acsami.7b11150.

[18] J.W. Maina, C.P. Gonzalo, A. Merenda, L. Kong, J.A. Schütz, L.F. Dumée, The growth of high density network of MOF nano-crystals across macroporous metal substrates – Solvothermal synthesis versus rapid thermal deposition, Appl. Surf. Sci. 427 (2018) 401–408. doi:10.1016/j.apsusc.2017.08.060.

[19] L.F. Dumée, L. He, B. Lin, F.M. Ailloux, J.B. Lemoine, L. Velleman, F. She, M.C. Duke, J.D. Orbell, G. Erskine, P.D. Hodgson, S. Gray, L. Kong, The fabrication and surface functionalization of porous metal frameworks-a review, J. Mater. Chem. A. 1 (2013) 15185–15206. doi:10.1039/c3ta13240d.

[20] K. V. Plakas, S.D. Sklari, D.A. Yiankakis, G.T. Sideropoulos, V.T. Zaspalis, A.J. Karabelas, Removal of organic micropollutants from drinking water by a novel electro-Fenton filter: Pilot-scale studies, Water Res. 91 (2016) 183–194. doi:10.1016/j.watres.2016.01.013.

[21] S. Garcia-Segura, E. Brillas, Advances in solar photoelectro-Fenton: Decolorization and mineralization of the Direct Yellow 4 diazo dye using an autonomous solar pre-pilot plant, Electrochim. Acta. 140 (2014) 384–395. doi:10.1016/j.electacta.2014.04.009.

[22] S. Garcia-Segura, E.B. Cavalcanti, E. Brillas, Mineralization of the antibiotic chloramphenicol by solar photoelectro-Fenton. From stirred tank reactor to solar pre-pilot plant., Appl. Catal. B Environ. 144 (2014) 588–598. doi:10.1016/j.apcatb.2013.07.071.

[23] A. El-Ghenymy, P.L. Cabot, F. Centellas, J.A. Garrido, R.M. Rodríguez, C. Arias, E. Brillas, Mineralization of sulfanilamide by electro-Fenton and solar photoelectro-Fenton in a pre-pilot plant with a Pt/air-diffusion cell, Chemosphere. 91 (2013) 1324–1331. doi:10.1016/j.chemosphere.2013.03.005.

[24] V.C. Sarasidis, K. V. Plakas, A.J. Karabelas, Novel water-purification hybrid processes involving in-situ regenerated activated carbon, membrane separation and advanced oxidation, Chem. Eng. J. 328 (2017) 1153–1163. doi:10.1016/j.cej.2017.07.084.

[25] B. Zhu, M. Duke, L.F. Dumée, A. Merenda, E. des Ligneris, L. Kong, P.D. Hodgson, S. Gray, Short review on porous metal membranes—Fabrication, commercial products, and applications, Membranes (Basel). 8 (2018). doi:10.3390/membranes8030083.

[26] C. Feng, Z. Yi, F. She, W. Gao, Z. Peng, C.J. Garvey, L.F. Dumée, L. Kong, Superhydrophobic and Superoleophilic Micro-Wrinkled Reduced Graphene Oxide as a Highly Portable and Recyclable Oil Sorbent, ACS Appl. Mater. Interfaces. 8 (2016) 9977–9985. doi:10.1021/acsami.6b01648.

[27] E.J. Ruiz, A. Hernández-Ramírez, J.M. Peralta-Hernández, C. Arias, E. Brillas, Application of solar photoelectro-Fenton technology to azo dyes mineralization: Effect of current density, Fe2+ and dye concentrations, Chem. Eng. J. 171 (2011) 385–392.

doi:10.1016/j.cej.2011.03.004.

[28] T.X.H. Le, R. Esmilaire, M. Drobek, M. Bechelany, C. Vallicari, S. Cerneaux, A. Julbe, M. Cretin, Nitrogen-Doped Graphitized Carbon Electrodes for Biorefractory Pollutant Removal, J. Phys. Chem. C. 121 (2017) 15188–15197. doi:10.1021/acs.jpcc.7b03100.

[29] J. Liu, Y. Qiao, C.X. Guo, S. Lim, H. Song, C.M. Li, Graphene/carbon cloth anode for high-performance mediatorless microbial fuel cells, Bioresour. Technol. 114 (2012) 275–280. doi:10.1016/j.biortech.2012.02.116.

[30] A.J. Bard, L.R. Faulkner, ELECTROCHEMICAL METHODS Fundamentals and Applications, 2001. doi:10.1016/B978-0-12-381373-2.00056-9.

[31] et al Ming. Wen, Haiqing. Liu, Amorphous FeNiPt nanoparticles with tunable length for electrocatalysis, Chem.Commun. (2009) 4530–4532. doi:0.1039/b907379e.

[32] T.X.H. Le, M. Bechelany, J. Champavert, M. Cretin, A highly active based graphene cathode for the electro-fenton reaction, RSC Adv. 5 (2015) 42536–42539. doi:10.1039/C5RA04811G.

[33] F. Qiang, L.L. Hu, L.X. Gong, L. Zhao, S.N. Li, L.C. Tang, Facile synthesis of super-hydrophobic, electrically conductive and mechanically flexible functionalized graphene nanoribbon/polyurethane sponge for efficient oil/water separation at static and dynamic states, Chem. Eng. J. 334 (2018) 2154–2166. doi:10.1016/j.cej.2017.11.054.

[34] T.X. Huong Le, B. Alemán, J.J. Vilatela, M. Bechelany, M. Cretin, Enhanced Electro-Fenton Mineralization of Acid Orange 7 Using a Carbon Nanotube Fiber-Based Cathode , Front. Mater. . 5 (2018) 9. https://www.frontiersin.org/article/10.3389/fmats.2018.00009.

[35] M. Panizza, M.A. Oturan, Degradation of Alizarin Red by electro-Fenton process using a graphite-felt cathode, Electrochim. Acta. 56 (2011) 7084–7087.

doi:10.1016/j.electacta.2011.05.105.

[36] T.X.H. Le, T. Van Nguyen, Z. Amadou Yacouba, L. Zoungrana, F. Avril, D.L. Nguyen, E. Petit, J. Mendret, V. Bonniol, M. Bechelany, S. Lacour, G. Lesage, M. Cretin, Correlation between degradation pathway and toxicity of acetaminophen and its by-products by using the electro-Fenton process in aqueous media, Chemosphere. 172 (2017) 1–9. doi:10.1016/j.chemosphere.2016.12.060.

[37] F.M. Allioux, O. David, A. Merenda, J.W. Maina, M.E. Benavides, A.P. Tanaka, L.F. Dumée, Catalytic nickel and nickel-copper alloy hollow-fiber membranes for the remediation of organic pollutants by electrocatalysis, J. Mater. Chem. A. 6 (2018) 6904–6915. doi:10.1039/c7ta11323d.